J. Indian Chem. Soc.,
Vol. 94, May 2017, pp. 457-468

Mycobacterium tuberculosis sterol 14α-demethylase inhibitor sulfonamides : Identified by high-throughput screening

Sayantan Pradhan and Chittaranjan Sinha*

Department of Chemistry, Inorganic Chemistry Section, Jadavpur University, Kolkata-700 032, India

E-mail : c_r_sinha@yahoo.com *Fax* : 91-33-2414658

Manuscript received 13 January 2017, accepted 07 February 2017

Abstract : Tuberculosis is a deadly infectious disease caused by *Mycobacterium tuberculosis*. Sterol 14α-demethylase cytochrome P450 51(CYP51) is a key target for antibiotic therapy. Azoles are used to disturb functional activity of CYP51 and thus promising antifungal agents. Sulfonamides, anti-microbial drug, also act as antifungal candidate. In this work high-throughput screening approach is used to find sulfonamides for lead candidate as CYP51 inhibitor. A library of 402 sulfonamides from various databases against *M. tuberculosis* CYP51 (CYP51Mt) are screened and has been examined the top binding hits for their inhibitory effects. Docking results show that binding affinity of newly searched ligands is higher than known tuberculosis drugs. Lipinski's rule of five protocols is followed to screen drug likeness and ADMET filtration is also used to value toxicity. DFT computation of optimized geometry and molecular orbitals have been used to correlate with the drug likeness. Pharmacophore generation is reported to recognize the binding patterns of inhibitors in the receptor active site. (2*R*)-2-(2,1,3-Benzothiadiazol-4-ylsulfonylamino)-*N*-[(1*S*,2*R*)-2-methylcyclohexyl]-2-phenylacetamide shows best theoretical efficiency. The compounds also bind to Adenine-Thymine region of tuberculosis Deoxyribonucleic acid (DNA). To observe the stability and flexibility of inhibitors the molecular dynamics simulation (MD) has been carried out.

Keywords : Sterol 14α-demethylase, structure based drug design, molecular docking, ADMET, pharmacophore, MD simulation.

Introduction

A major population in the second decade of 21st Century is still infected with *Mycobacterium tuberculosis* (MTB)[1]. Present treatment protocol and use of drugs need thorough improvement. Therefore, progress for new drug design strategies are urgently needed to fight against tuberculosis (TB) and especially to the multidrug resistant TB (MDR-TB)[2]. Recent studies have shown that genome of MTB has a large number of open reading frame (ORF) those are related to known sterol biosynthetic enzymes[3]. Sterol 14α-demethylase (Fig. 1), a fungal enzyme, is inhibited by azole compounds[4]. Several azoles have been documented against *M. smegmatis*, *M. tuberculosis* H37Ra and *Streptomyces coelicotar*[5]. These drugs act on multiple targets in mycobacteria and recent studies have demonstrated that azole drugs inhibit the biosynthesis of glycol peptide lipids (GPLs), which in turn are responsible for maintaining the integrity of the mycobacterial cell envelope[6,7].

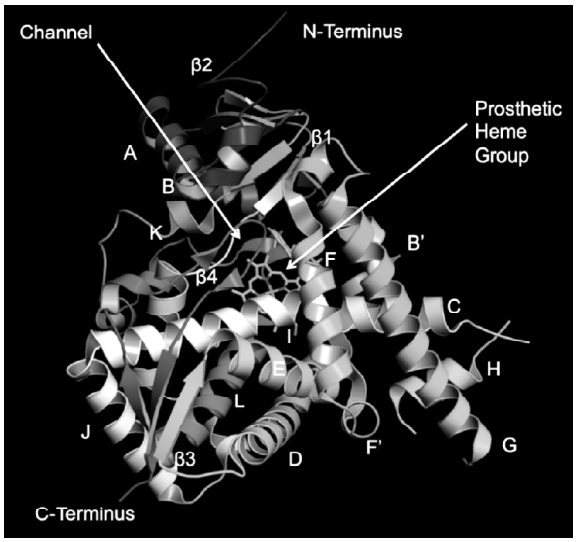

Fig. 1. Structure of lanosterol 14α-demethylase (CYP51).

Azoles are currently the most widely used and studied class of antifungals[8]. These azole compounds bind as the sixth ligand to the heme group in CYP51, thereby altering

the structure of the active site and acting as noncompetitive inhibitors[9]. However, persistent use of azoles as antifungal drug has resulted in the emergence of drug resistance among certain fungal strains[10]. On the otherhand sulfonamides, anti-microbial drugs, shows activity against MTB[11,12]. Since the best docked sulfonamide binds to the heme group in CYP51 of *M. tuberculosis* and surrounding amino acids are almost same as azole drugs, it can be assumed that sulfonamides can be used in place of azole drugs[8].

In this work, sulfonamides are docked with protein CYP51 (MTB), obtained from Protein Data Bank (PDB id : 2CIB) and searched to predict potential drugs against *M. tuberculosis*. So far, 504 similar compounds are traced and 402 of them are passed Lipinski's filter. Amongst the 402 compounds, (2*R*)-2-(2,1,3-benzothiadiazol-4-ylsulfonylamino)-*N*-[(1*S*,2*R*)-2-methylcyclohexyl]-2-phenylacetamide (Ligand) shows best docking efficiency. It is also passed the ADMET filter for reviewing its toxicity. Six best docked compounds are taken into consideration. Quantum chemistry calculation, pharmacophore generation, molecular dynamics simulation and Quantitative structure-activity relationship (QSAR) have been carried out to observe stability, persistence properties of best docked molecule.

Experimental methodology

Sequence alignment analysis :

The procedure of detecting the functional resemblance between two or more sequences of amino acids by concurrently aligning the sequences was called multiple sequence alignment (MSA) and is important for finding the functionality of proteins and evolution history of the species[13]. Sterol 14α-demethylase (CYP51) enzymes have also found in human body but their functions are different from that of Mtbs; the mammalian cell is not sensitive to sterol 14α-demethylase[14]. Using target validation protocol these molecules have been validated as potential drug and not harmful to human health[15]. To identify the homology and relationship between human sterol 14α-demethylase and Mtb sterol 14α-demethylase, sequence comparison was performed using multiple sequence alignment in Clustal omega[16].

High throughput virtual screening (HTVS) :

From large number of sulfonamides, lead molecules may be selected by High Throughput Screening (HTS) by performing individual biochemical assays but to save huge cost and time incorporation of economical and effective computational methodology namely virtual High Throughput Screening (vHTS) is done in *in silico* drug design. HTS is a computational screening method which is widely applied to screen from libraries of *in silico* drug like compounds to check the binding affinity of the target receptor with the library compounds[17]. HTS is done by docking which is accomplished by using various scoring function which computes the binding affinity of the target receptor with the compounds. HTS and vHTS are complementary methods and vHTS has been shown to reduce false positives in HTS[18,19].

Docking of 402 compounds have been done by Autodockvina on windows platform on 8 G.B, R.A.M computer with Intel I 5 processor[20]. The crystallographic co-ordinates for sterol 14α-demethylase was retrieved from the Protein Data Bank (PDB id : 2CIB). Before docking procedure, protein structures were prepared by using Discovery Studio 4 software's protein preparation wizard. Following which, loops were built, protonation were done and hydrogen atoms were added to the crystal structures. Active site of the protein was within the grid dimensions of $30\times30\times30$ Å^3. Amongst the docked conformations, one which bound with high affinity at the active site was visualized (Fig. 2) for detailed ligand-protein interactions in Discover Studio Visualizer 4.0.

Drug likeness :

The drug likeness perception is a useful guideline for early stage drug discovery[21]. Investigation of the observed distribution of some key physicochemical attributes of approved drugs, including molecular weight, hydrophobicity and polarity, reveals that the drugs favorably occupy a range those are described as "druglike"[21]. Calculation of drug likeness is most commonly manifested as rules, the original and most well-known of which is Lipinski's Rule of Five 5(Ro5) and Ghose's rule[22,23]. The Lipinski's rule states that a compound is more likely to exhibit druglike physicochemical attributes if the criteria are fulfilled : Molecular weight of less than 500 Dalton and the number of hydrogen bond donors is less than 5, the number of hydrogen bond acceptors is less than 10 and log P values each less than 5[22]. The Ghose rule states that, log P should be in –0.4 to +5.6 range, molar refrac-

tivity should be from 40 to 130, molecular weight should be from 180 to 500, number of atoms should be from 20 to 70, polar surface area no greater than 140 Å[23]. Drug likeness was completed by Discovery Studio 4 on windows platform on 8 G.B, R.A.M computer with Intel I 5 processor.

ADMET properties :

Nowadays evaluation of drug metabolism, pharmacokinetics and toxicity were done much earlier stage of drug design[24]. In the era of virtual screening demand of data dramatically increased, so have the demands for large quantities of early statistics on absorption, distribution, metabolism, excretion (ADME) and toxicity data (ADMET)[25].

Qualitative classification models were applied for ADMET prediction, which were established using support vector machine classification algorithm and in house substructure pattern recognition method[26]. By using support vector machine regression algorithm, some quantitative regression models were also constructed and implemented. The strength of model was validated based on cross validation, and the predictability of several models was validated using available external validation sets[27]. ADMET properties of best docked molecule were done by Discovery Studio 4 and support vector machine regression algorithm on windows platform on 8 G.B, R.A.M computers with Intel I 5 processor.

Quantum chemistry calculation :

Electronic structure (molecular orbital) and the effect of substituent of druglike molecules has major role in the drug proficiency[28]. A molecular orbital (MO) defines the wavelike conduct of an electron in a molecule its function can be used to calculate chemical and physical attributes such as the probability of finding an electron in any definite area[29]. The highest occupied molecular orbital and lowest unoccupied molecular orbital are often referred to as the HOMO and LUMO, respectively. The difference of the energies of the HOMO and LUMO, termed the band gap, may use to calculate the molecular reactivity, strength and stability of the complexes[30].

DFT (Density functional theory) computation was done by Gaussian 09W on windows platform on 8 G.B, R.A.M computer with Intel I 5 processor for HOMO-LUMO band gap[31]. Gaussian calculation has been done in Gaussian 09 panel using Becke's three-parameter exchange potential and Lee-Yang-Parr correlation functional (B3LYP) theory with basis set 6-31G[32–34]. After that, surfaces (molecular orbital, density, potential) and electrostatics potential charges (EPS) were used to analyze the highest occupied molecular orbital (HOMO) and lowest unoccupied molecular orbital (LUMO).

Drug-DNA interaction :

Deoxyribonucleic acid (DNA) and druglike molecular interaction has become an active research area at the interface between chemistry, molecular biology and medicine[35]. Most of the drugs are groove binders for a tight fit to the drug[36]. A group of heterocyclic or aromatic hydrocarbon rings act as minor groove binding molecules which allows the displacement of water and the molecule fits into the minor groove[37]. Through hydrophobic interactions and hydrogen bonding, drugs interact with adenine thymine (AT) rich regions of DNA in the minor groove[38]. The terminal adenine group of DNA is basic in nature and attracts the druglike molecule to the negatively charged DNA phosphodiester backbone[36]. To find the binding pattern ligand (best docked molecule) with Mtb DNA (PDB id : 3pvv) docking method was used. Transcription and replication which are vital jobs of DNA, vital to cell survival and production, were affected by the interaction of exogenous agents and the DNA function could be artificially modulated[38]. Drug DNA docking was done by AutoDockvina on windows platform on 8 G.B, R.A.M computer with Intel I 5 processor.

Quantitative structure-activity relationship (QSAR) : (MLR) :

QSAR is used for quantitative correlation of physicochemical attributes of ligands. It is widely used tool, ominously contributing to the drug discovery process[39]. Multiple Linear Regression (MLR) is used as a chemo-metric QSAR technique for variable selection and statistical fit in and uses a group of random variables and tries to find a mathematical association among them[40]. We observed MLR of 7 molecules (structure analogues –10.7 to –10.6). We took drug likeness properties (Molecular weight, hydrogen acceptor, hydrogen donor and log P) of these molecules serve as independent variable and docking score is dependent variable for MLR. The MLR calculation was carried out by windows platform on 8 G.B, R.A.M computer with Intel I 5 processor[41].

Pharmacophore generation :

Interactions between the druglike molecules and their target proteins are retrieved by docking results. Receptor ligand interactions determined by chemical structure and functionalities, bonds, and their location flexibility towards each other[42]. Pharmacophore model describes chemical attributes that make a druglike molecule active towards its target. In these models, chemical attributes are represented as called pharmacophore features, they are acquired either from a set of active compounds or directly from the observed protein ligand interactions[42]. In the present work pharmacophore generation executed by receptor ligand pharmacophore generation with Discovery Studio 4 for study the interactions between protein and ligand on windows platform on 8 G.B, R.A.M computer with Intel I 5 processor.

Molecular dynamics simulation :

Molecular dynamics (MD) simulations approaches used for structural flexibility of the overall drug protein model system and to estimate of the thermodynamics and kinetics associated with drug protein recognition and binding[43]. It helps optimizing protein affinity and drug dwelling time toward improved drug efficiency[43]. MD simulation was calculated to further confirm the interaction strength and stability of the receptor-ligand complex determined from molecular docking by discovery studio's standard dynamics cascade wizard on windows platform on 8 G.B, R.A.M computer with Intel I 5 processor.The same PDB file (2CIB) which was modified for docking and best docked molecule were taken as protein-ligand complexes. Before performing MD simulations, Charm force field was applied to each of the protein-ligand complexes and solvation was set to explicit periodic boundary[44]. The total production time of 40 pico seconds (ps) simulations were performed with default setting.

Results and discussion

Selection of lead drug :

Importance of functional group, size, number of H-bond donors and acceptors in a compound are useful in the study to dock in the active domain of CYP51 protein. Azoles are promising antifungal agents and dock in the cavity of CYP51. Sulfonamides are also analogously active as antifungal candidate. So we have selected 402 sulfonamides from library through high-throughput screening approach to find lead candidate as CYP51 inhibitor.

Sequence alignment analysis :

Sequence alignment analysis result showed that there is no significant match between human and *M. tuberculosis* sterol 14α-demethylase (CYP51). Similarity between human and *M. tuberculosis* sterol 14α-demethylase is less than 33%, there is no functional similarities between them (Table 1). PDB id 3LD6, 3JUV, 3JUS are human sterol 14α-demethylase and other than PDB id all are *M. tuberculosis* sterol 14α-demethylase. By viewing the result summary of clustal omega, that 3LD6, 3JUV, 3JUS showing 100% similarity, with human sterol 14α-demethylase the similarities are less than 33% (Table 1).

High throughput virtual screening (HTVS) :

Ligands were docked in the active site of sterol 14α-demethylase *M. tuberculosis*. Among the ligands the best docked molecule is (2*R*)-2-(2,1,3-benzothiadiazol-4-ylsulfonylamino)-*N*-[(1*S*,2*R*)-2-methylcyclohexyl]-2-phenylacetamide which forms 2 hydrogen bonds with amino acids of the sterol 14α-demethylase at 2.32883 Å and 2.55385 Å (Table 1, Fig. 2). The hydrogen bond forming amino acids are histidine (HIS) 259 and alanine (ALA) 256. Ligand also forms two hydrophobic interactions with amino acids of the sterol 14α-demethylase at 3.75359 Å and 3.82126 Å (Table 2, Fig. 2). The docking score (binding affinity) is –10.7 kcal/mol, better than approved TB drugs like drugs-*p*-amino salicylic acid (PAS, binding affinity, –8.9 kcal/mol) and ethambutol (binding affinity, –7.8 kcal/mol). The ligand has surrounding amino acids those are almost same as azole drugs like Fluconazole (Table 3).

Drug likeness and ADMET :

Six molecules along with best docked candidate are passed Lipinski's rule of five and Ghose's rule (Supplementary material). ADMET is used to determine permeability for BBB (blood-brain barrier), HIA (human intestinal absorption), P-glycoprotein Substrate Inhibitor, renal organic cation transporter, etc. (Table 4). The result shows that the ligand is positive (+) in Human Intestinal Absorption, Blood-Brain Barrier which means the molecule is well absorbed in human body (Table 4) and would not cross blood brain barrier[27]. Inhibition and initiation of P-glycoprotein had been reported as the causes of drug-

Table 1. Showing Clustal omega result

Sl. no.	PDB ID and chain	Enzymes	Similarities in percentage (%)				
1.	3LD6_A	Human lanosterol 14alpha-demethylase_A	100	100	100	100	100
2.	3LD6_B	Human lanosterol 14alpha-demethylase_B	100	100	100	100	100
3.	3JUV_A	Hum lanosterol 14alpha-demethylase _A	100	100	100	100	100
4.	3JUS_A	Hum lanosterol 14alpha-demethylase _A	100	100	100	100	100
5.	3JUS_B	Hum lanosterol 14alpha-demethylase _B	100	100	100	100	100
6.	1H5Z_A	MTB lanosterol 14alpha-demethylase _A	32.14	32.14	32.14	32.14	32.14
7.	1EA1_A	MTB lanosterol 14alpha-demethylase _A	32.14	32.14	32.14	32.14	32.14
8.	1E9X_A	MTB lanosterol 14alpha-demethylase _A	32.14	32.14	32.14	32.14	32.14
9.	1U13_A	MTB lanosterol 14alpha-demethylase _A	31.92	31.92	31.92	31.92	31.92
10.	2W09_A	MTB lanosterol 14alpha-demethylase _A	32.14	32.14	32.14	32.14	32.14
11.	2W0B_A	MTB lanosterol 14alpha-demethylase _A	32.14	32.14	32.14	32.14	32.14
12.	2VKU_A	MTB lanosterol 14alpha-demethylase _A	32.14	32.14	32.14	32.14	32.14
13.	2CIB_A	MTB lanosterol 14alpha-demethylase _A	32.14	32.14	32.14	32.14	32.14
14.	2CI0_A	MTB lanosterol 14alpha-demethylase _A	32.14	32.14	32.14	32.14	32.14
15.	2BZ9_A	MTB lanosterol 14alpha-demethylase _A	32.14	32.14	32.14	32.14	32.14
16.	2BZ9_B	MTB lanosterol 14alpha-demethylase _B	32.14	32.14	32.14	32.14	32.14
17.	1X8V_A	MTB lanosterol 14alpha-demethylase _A	32.14	32.14	32.14	32.14	32.14
18.	2W0A_A	MTB lanosterol 14alpha-demethylase _A	31.92	31.92	31.92	31.92	31.92

drug interaction[45]. The best docked molecule was P-glycoprotein non-inhibitor, in the result, that implies that the best docked molecule won't interact with other drugs. Organic cation transporters are responsible for drug absorption and disposition in the kidney, liver, and intestine[46]. ADMET result of best docked molecule shows that it was non-inhibitor of renal organic cation transporter. The human cytochromes P450 (CYPs), particularly isoforms 1A2, 2C9, 2D6, and 3A4, are responsible for about 90% oxidative metabolic reactions. Inhibition of CYP enzymes will lead to inductive or inhibitory failure of drug metabolism[47,48] and the best docked molecule is non-inhibitor/substrate, so it would not a barrier in drug metabolism.

The Ames test is a widely employed method that uses bacteria to test whether a given chemical can cause cancer[49]. ADMET result shows two best docked molecules were non-Ames toxic and non-carcinogenic.

Human Ether-à-go-go-Related Gene (hERG) is a gene sensitive to drug binding[50]. ADMET result shows best docked molecule was weak inhibitor and non-inhibitor of hERG inhibition (predictor I and II) which means best docked molecule will be well bind well with receptor[50].

Quantum chemistry calculation :

The plots of HOMO and LUMO show the positive electron density in red color and negative electron density in green (Fig. 3A and 3B). The selected drug candidates showed minimal HOMO-LUMO gap with the energy difference of –0.13638 eV, signifying molecular reactivity.

Fig. 3A and 3B show that HOMO and LUMO of ligand. Plots of highest occupied molecular orbital (HOMO) and lowest unoccupied molecular orbital (LUMO) of ligand. The positive electron density has been shown in pink color while negative have been shown in green.

Drug-DNA interaction :

The best docked molecule is docked in to the adenine-thymine (AT) rich sequences minor groove of tuberculosis DNA by hydrogen bonding (Fig. 4). Its formation of hydrogen bonds to DNA bases like to 'O' of thymine and also its specificity towards adenine-thymine (AT) rich sequences was like other groove binder drugs[35]. The ligand was bound to minor groove of Mtbs DNA. Ligand was bound DNA by hydrogen bonds ranging from 2.60861 Å to 5.62963 Å (Table 5).

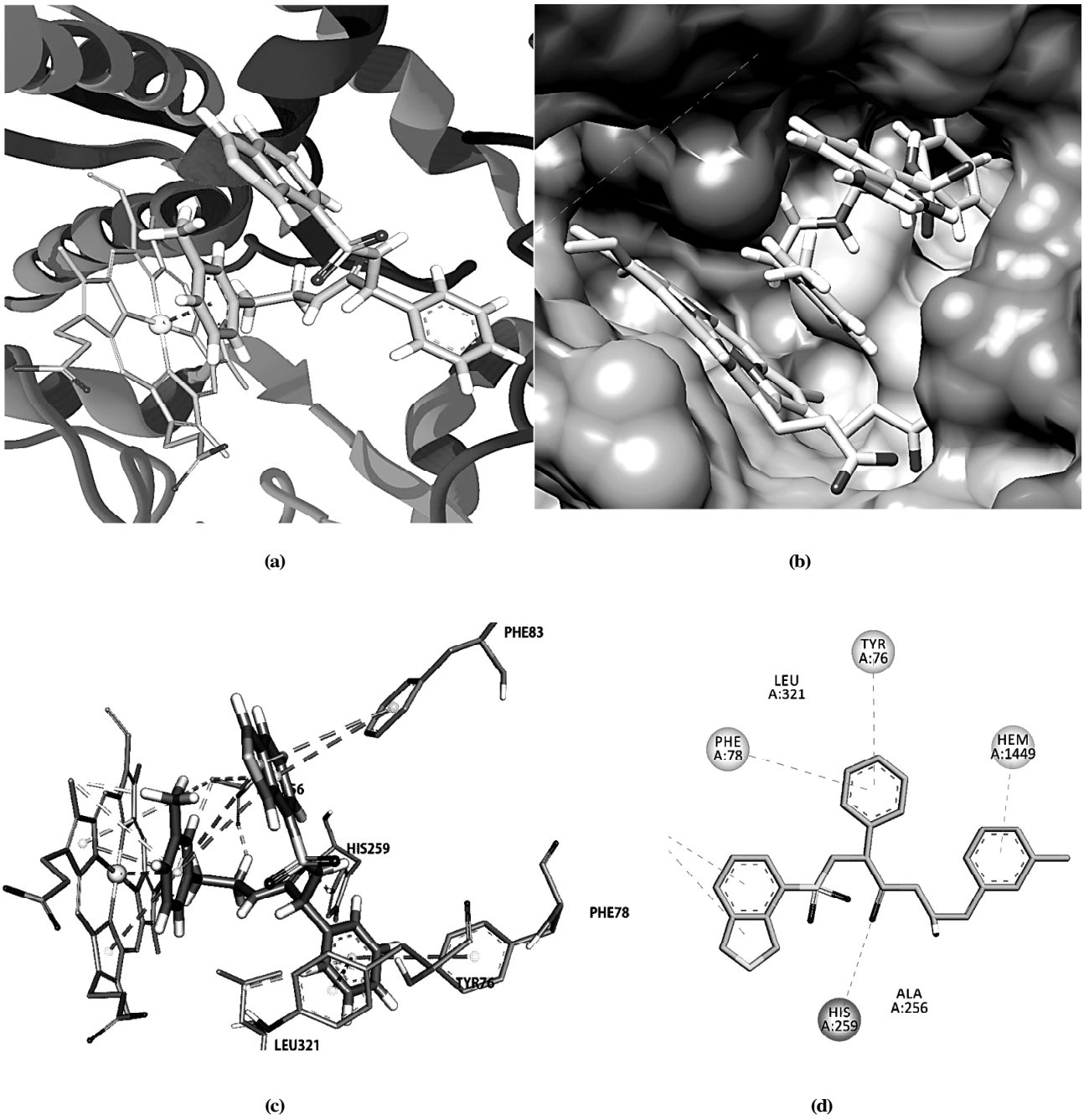

Fig. 2. Comprehensive perception of sterol 14α-demethylase and (2*R*)-2-(2,1,3-benzothiadiazol-4-ylsulfonylamino)-*N*-[(1*S*,2*R*)-2-methylcyclohexyl]-2-phenylacetamide interaction after docking. (a) Shows that (2*R*)-2-(2,1,3-benzothiadiazol-4-ylsulfonylamino)-*N*-[(1*S*,2*R*)-2-methylcyclohexyl]-2-phenylacetamide is docked in active site of sterol 14α-demethylase. Secondary structure of sterol 14α-demethylase represented by and ribbon and (2*R*)-2-(2,1,3-benzothiadiazol-4-ylsulfonylamino)-*N*-[(1*S*,2*R*)-2-methylcyclohexyl]-2-phenylacetamide is represented by stick model. (b) Shows that surface model of the same picture where structure of sterol 14α-demethylase represented by and surface. (c) (2*R*)-2-(2,1,3-Benzothiadiazol-4-ylsulfonylamino)-*N*-[(1*S*,2*R*)-2-methylcyclohexyl]-2-phenylacetamide surrounding amino acids were shown in the picture. Interactions of ligand with 14α-demethylase amino acids, ligand surrounding amino acids are in three letters code represented in dark blue. (d) Same picture represented in 2D format.

Table 2. Bonds between ligand and sterol 14α-demethylase

Bond name	Distance (Å)	Bond category	Bond type
A:HIS259:HE2 - :LIGAND:O	2.32883	Hydrogen bond	Conventional hydrogen bond
LIGAND:H9 - A:ALA256:O	2.55385	Hydrogen bond	Carbon hydrogen bond
A:HEM1449 - :LIGAND	3.75359	Hydrophobic	Pi-Pi Stacked
A:HEM1449:CMD - :LIGAND:C	3.82126	Hydrophobic	Alkyl

Table 3. Surrounding amino acids of the ligands

PDB ligand	Azole drug (Fluconazole)	Best docked compound
TYR76	TYR76	TYR76
PHE78	PHE78	PHE78
PHE83	ARG96	PHE83
ALA256	ALA256	ALA256
LEU321	THR260	HIS259
	LEU321	LEU321

Table 4. ADMET properties of ligand

ADMET Predicted Profile	Result	Probability
Classification model		
Blood-Brain barrier	BBB+	0.6153
Human intestinal absorption	HIA+	0.9938
P-Glycoprotein inhibitor	Non-inhibitor	0.7958
	Non-inhibitor	0.7580
Renal organic cation	Non-inhibitor	0.8561
Transporter		
Metabolism		
CYP450 2C9 substrate	Non-substrate	0.5000
CYP450 2D6 substrate	Non-substrate	0.8265
CYP450 3A4 substrate	Non-substrate	0.5703
CYP450 1A2 inhibitor	Non-inhibitor	0.7883
CYP450 2C9 inhibitor	Non-inhibitor	0.5316
CYP450 2D6 inhibitor	Non-inhibitor	0.8793
Toxicity		
Human Ether-à-go-go-Related	Weak inhibitor	0.9599
Gene inhibition	Non-inhibitor	0.7486
AMES toxicity	Non-AMES toxic	0.7287
Carcinogens	Non-carcinogens	0.8439

Quantitative structure-activity relationship (QSAR) and pharmacophore generation :

The MLR result has shown that R value is 0.826 and R^2 is 0.682. The values of R and R^2 are close to +1, and so implies positive and good correlation between drug likeness and docking score[40]. 68.2% of the change can be explained by the change in the 4 independent variables. We could assume that docking score is changing along with drug likeness properties.

The generated pharmacophore models based on receptor-ligand interactions by docking have confirmed all major interactions in the drug-receptor interaction modes (Fig. 5). The number of features, feature set, and selectivity score from pharmacophore generation were observed from the best docked molecule. Fig. 5 showed the pharmacophore map of (2*R*)-2-(2,1,3-benzothiadiazol-4-ylsulfonylamino)-*N*-[(1*S*,2*R*)-2-methylcyclohexyl]-2-phenylacetamide.

Molecular dynamics simulation :

The MD simulation study of best docked molecule, (2*R*)-2-(2,1,3-benzothiadiazol-4-ylsulfonylamino)-*N*-[(1*S*,2*R*)-2-methylcyclohexyl]-2-phenylacetamide with *Mycobacterium tuberculosis* sterol 14α-demethylase were done for 40 ps and ten thousand steps. Same procedure done for thirteen thousand steps and 40 ps. MD production run and the trajectory of the various energy profiles was created and analyzed. Bond energy and root-mean-square deviation of atomic positions (R.M.S.D or simply root-mean-square deviation) of (2*R*)-2-(2,1,3-benzothiadiazol-4-ylsulfonylamino)-*N*-[(1*S*,2*R*)-2-methylcyclohexyl]-2-phenylacetamide with sterol 14α-demethylase shown in Figs. 5, 6 respectively. Total energy after MD simulation was –18,209.3 kcal/mol. As the graph showed that for the best docked molecule the bond strength were increased from initial protein. So it can was clearly predicted that molecule formed stable conformation with *Mycobacterium tuberculosis* sterol 14α-demethylase. Superimposed structures of first, middle and last conformation of *Mycobacterium tuberculosis* sterol 14α-demethylase shows the deviation of end point of the dynamics from the initial point of dynamics (Fig. 8), deviation of the middle and last conformation from the starting conformation can be clearly visible from the figure.

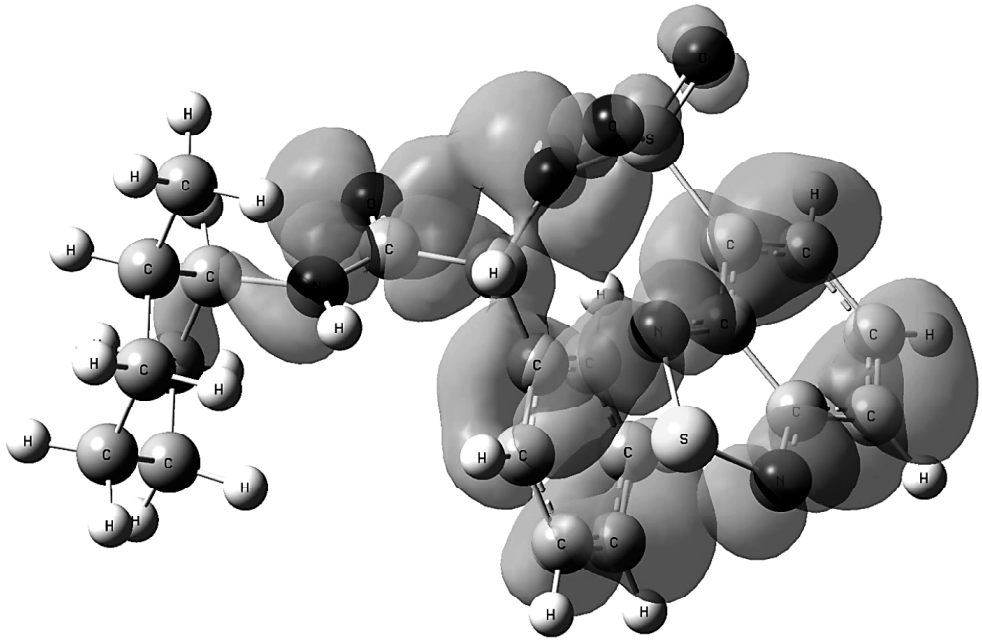

Fig. 3A. HOMO, E (HOMO) = –0.24455 eV.

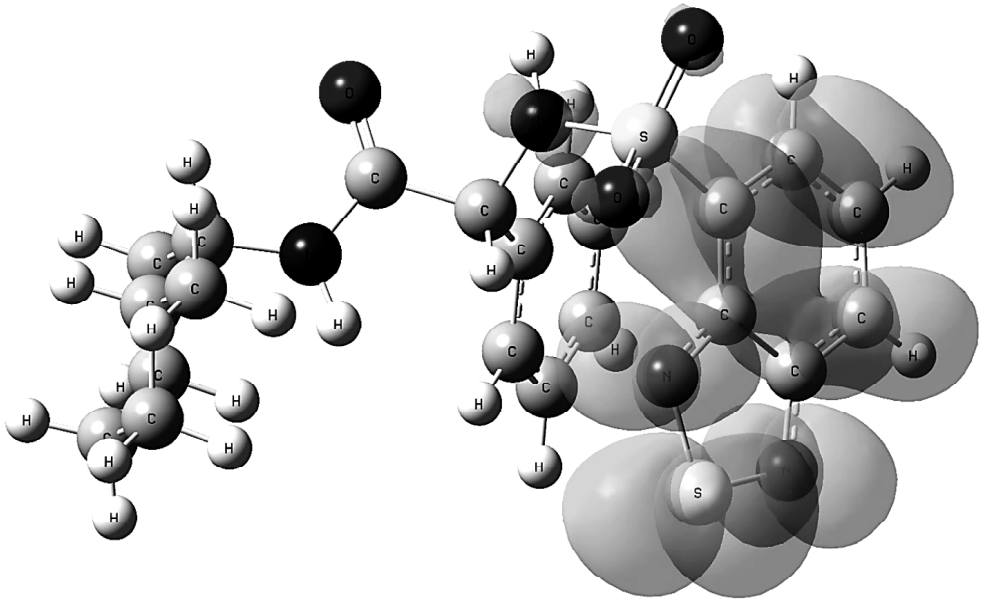

Fig. 3B. LUMO, E (LUMO) = –0.10817 eV.

Table 5. Bonds between ligand and Mtbs DNA

Bond name	Distance (Å)	Bond category	Bond type
LIGAND:H22 - C:DT104:O2	2.60861	Hydrogen bond	Conventional hydrogen bond
C:DG105:N2 - :LIGAND	3.95208	Hydrogen bond	Pi-Donor hydrogen bond
LIGAND:S - D:DA211	5.28209	Other	Pi-Sulfur
LIGAND:S - D:DA210	5.62963	Other	Pi-Sulfur

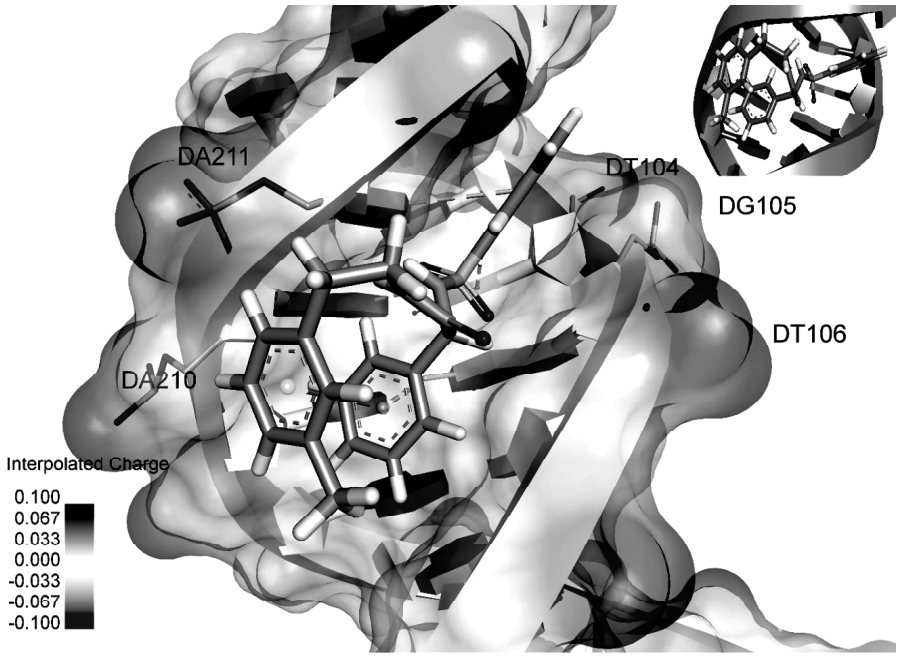

Fig. 4. Interaction between best docked molecule (Ligand) and Mtbs DNA. (a) Shows that best docked molecule docked (represented in stick) in the minor groove of tuberculosis DNA (represented by surface model). (b) Shows that same picture where tuberculosis DNA is represented in ladder model.

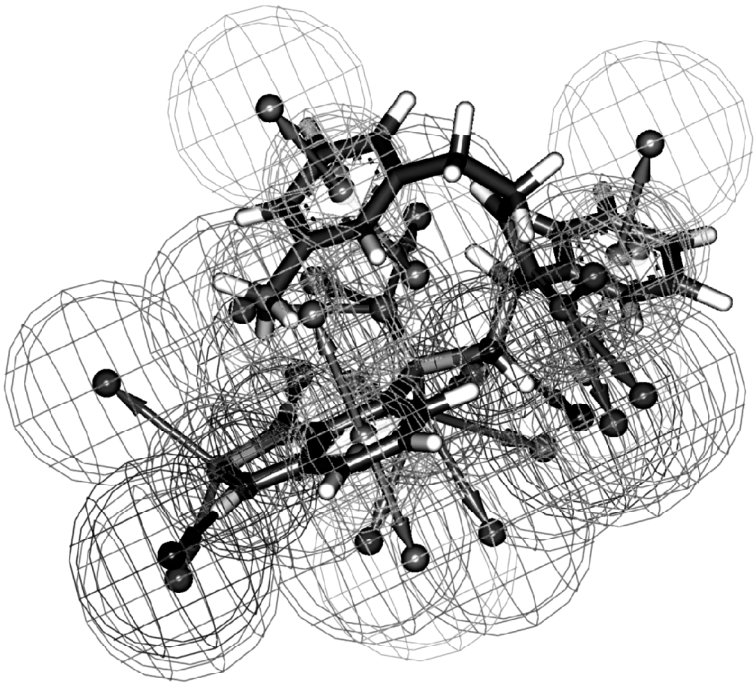

Fig. 5. Pharmacophore features of (2*R*)-2-(2,1,3-benzothiadiazol-4-ylsulfonylamino)-*N*-[(1*S*,2*R*)-2-methylcyclohexyl]-2-phenylacetamide based on receptor-ligand pharmacophore generation. The hydrogen bond acceptor, hydrogen bond donor, positive ionizable feature and negative ionizable features are shown as green, magenta, orange, and blue, respectively.

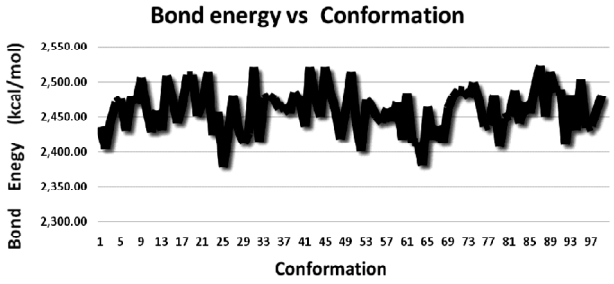

Fig. 6. Shows bond energy graph of (2*R*)-2-(2,1,3-benzothiadiazol-4-ylsulfonylamino)-*N*-[(1*S*,2*R*)-2-methylcyclohexyl]-2-phenylacetamide. X axis showing bond energy and y axis showing number of conformation that were visited during the simulation.

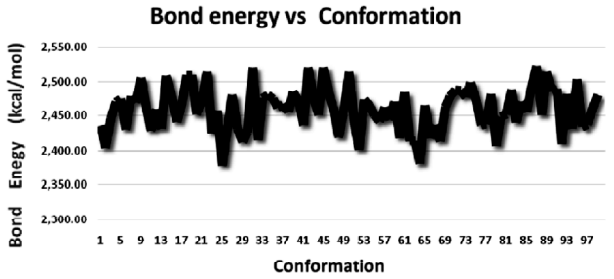

Fig. 7. Shows R.M.S.D graph of (2*R*)-2-(2,1,3-benzothiadiazol-4-ylsulfonylamino)-*N*-[(1*S*,2*R*)-2-methylcyclohexyl]-2-phenylacetamide. X axis showing R.M.S.D and y axis showing number of conformations. All RMSD values are calculated with respect to the starting conformation.

Fig. 8. Shows results of molecular dynamics, last conformation (structure) superimposed (coloured in pink) with first conformation (coloured in brown) middle conformation (coloured in blue) of *Mycobacterium tuberculosis* sterol 14α-demethylase.

Conclusion

Sulfonamides, anti-microbial agent, active against Mtbs *in vivo*. The best docked compound, (2*R*)-2-(2,1,3-benzothiadiazol-4-ylsulfonylamino)-*N*-[(1*S*,2*R*)-2-methylcyclohexyl]-2-phenylacetamide, shows higher score than approved TB drugs-*p*-amino salicylic acid (PAS) and ethambutol. ADMET properties also approve easy crossing of blood brain barrier section. Since the best docked compound bind to the heme group in CYP51 of *Mycobacterium tuberculosis* and surrounding amino acids are almost same as azole drugs, it can be assumed that sulfonamides can be used in place of azole drugs. Most of the sulfonamides have passed through ADMET and drug like properties filtration successfully and quantum chemistry, MD calculation shows best docked molecules interaction pattern and stability, so sulfonamide derivatives have potential of being a good drug.

Acknowledgement

We sincerely thank Department of Science and Technology, Kolkata, West Bengal, India [Grant number 228/1(10)/(Sanc.)/ST/P/S&T/9G-16/2012] and University Grants Commission, New Delhi, India [Grant number F. 42-333/2013(SR)] for funding.

References

1. G. K. Sandhu, *J. Glob. Infect. Dise.*, 2011, **3**, 143.
2. H. S. Cox, J. J. Furin, C. D. Mitnick, C. Daniels, V. Cox and E. Goemaere, *Bull. World Health Org.*, 2015, **93**, 491.
3. G. I. Lepesheva and M. R. Waterman, *Biochim. Biophys. Acta*, 2007, **1770**, 467.
4. M. A. Ghannoum and L. B. Rice, *Clin. Microb. Rev.*, 1999, **12**, 501.
5. Z. Sun and Y. Zhang, *J. Int. Union Tube. Lung Dis.*, 1999, **79**, 319.
6. K. J. McLean, K. R. Marshall, A. Richmond, I. S. Hunter, K. Fowler, T. Kieser, S. S. Gurcha, G. S. Besra and A. W. Munro, *Microb.*, 2002, **148**, 2937.
7. P. Burguiere, J. Fert, I. Guillouard, S. Auger, A. Danchin and I. Martin-Verstraete, *J. Bact.*, 2005, **187**, 6019.
8. J. G. Mullins, J. E. Parker, H. J. Cools, R. C. Togawa, J. A. Lucas, B. A. Fraaije, D. E. Kelly and S. L. Kelly, *PLoS One*, 2011, **6**, 20973.
9. D. J. Sheehan, C. A. Hitchcock and C. M. Sibley, *Clini. Microb. Rev.*, 1999, **12**, 40.

10. W. Ong, A. Sievers and D. E. Leslie, *Antimicrob. Agents Chemoth.*, 2010, **54**, 2748.
11. W. D. Ihlenfeldt, E. E. Bolton and S. H. Bryant, *J. Cheminfo.,* 2009, **1**, 20.
12. J. J. Irwin and B. K. Shoichet, *J. Chem. Info. Model.*, 2005, **45**, 177.
13. S. F. Altschul, *J. Theo. Bio.*, 1989, **138**, 297.
14. W. D. Nes, *Chem. Rev.*, 2011, **111**, 6423.
15. L. M. Podust, J. P. von Kries, A. N. Eddine, Y. Kim, L. V. Yermalitskaya, R. Kuehne, H. Ouellet, T. Warrier, M. Altekoster, J. S. Lee, J. Rademann, H. Oschkinat, S. H. Kaufmann and M. R. Waterman, *Antimicrob. Agents Chemoth.*, 2007, **51**, 3915.
16. R. R. Rani and D. Ramyachitra, *Bio Syst.,* 2016, **150**, 177.
17. B. K. Shoichet, *Nature*, 2004, **432**, 862.
18. J. Bajorath, *Nature Rev. Drug Discovery*, 2002, **1**, 882.
19. J. L. Jenkins, R. Y. Kao and R. Shapiro, *Proteins*, 2003, **50**, 81.
20. O. Trott and A. J. Olson, *J. Comp. Chem.*, 2010, **31**, 455.
21. G. R. Bickerton, G. V. Paolini, J. Besnard, S. Muresan and A. L. Hopkins, *Nature Chem.*, 2012, **4**, 90.
22. C. A. Lipinski, F. Lombardo, B. W. Dominy and P. J. Feeney, *Adv. Drug Deliv. Rev.*, 2001, **46**, 3.
23. A. K. Ghose, V. N. Viswanadhan and J. J. Wendoloski, *J. Comb. Chem.,* 1999, **1**, 55.
24. S. Pandey, P. Pandey, G. Tiwari and R. Tiwari, *Pharma. Methods*, 2010, **1**, 14.
25. T. Lei, Y. Li, Y. Song, D. Li, H. Sun and T. Hou, *J. Cheminf.*, 2016, **8**, 6.
26. H. van de Waterbeemd and E. Gifford, *Drug Disc.*, 2003, **2**, 192.
27. J. Shen, F. Cheng, Y. Xu, W. Li and Y. Tang, *J. Chem. Inf. Model.,* 2010, **50**, 1034.
28. A. B. Rozhenko, *Springer Netherlands*, 2014, **17**, 207.
29. C. Steinmann, D. G. Fedorov and J. H. Jensen, *PLoS One*, 2012, **7**, 41117.
30. K. Fukui, T. Yonezawa and H. Shingu, *J. Chem. Phys.,* 1952, **20**, 722.
31. M. J. Frisch, G. W. Trucks, H. B. Schlegel, G. E. Scuseria, M. A. Robb, J. R. Cheeseman, G. Scalmani, V. Barone, B. Mennucci, G. A. Petersson, H. Nakatsuji, M. Caricato, X. Li, H. P. Hratchian, A. F. Izmaylov, J. Bloino, G. Zheng, J. L. Sonnenberg, M. Hada, M. Ehara, K. Toyota, R. Fukuda, J. Hasegawa, M. Ishida, T. Nakajima, Y. Honda, O. Kitao, H. Nakai, T. Vreven, J. A. Montgomery (Jr.), J. E. Peralta, F. Ogliaro, M. J. Bearpark, J. Heyd, E. N. Brothers, K. N. Kudin, V. N. Staroverov, R. Kobayashi, J. Normand, K. Raghavachari, A. P. Rendell, J. C. Burant, S. S. Iyengar, J. Tomasi, M. Cossi, N. Rega, N. J. Millam, M. Klene, J. E. Knox, J. B. Cross, V. Bakken, C. Adamo, J. Jaramillo, R. Gomperts, R. E. Stratmann, O. Yazyev, A. J. Austin, R. Cammi, C. Pomelli, J. W. Ochterski, R. L. Martin, K. Morokuma, V. G. Zakrzewski, G. A. Voth, P. Salvador, J. J. Dannenberg, S. Dapprich, A. D. Daniels, Ö. Farkas, J. B. Foresman, J. V. Ortiz, J. Cioslowski and D. J. Fox, Gaussian 09, Gaussian, Inc., 2009.
32. A. D. Becke, *J. Chem. Phys.*, 1993, **98**, 5648.
33. P. M. W. Gill, B. G. Johnson, J. A. Pople and M. J. Frisch, *Chem. Phys. Lett.*, 1992, **197**, 499.
34. F. J. Devlin, J. W. Finley, P. J. Stephens and M. J. Frisch, *J. Phys. Chem.*, 1995, **99**, 16883.
35. M. Sirajuddin, S. Ali and A. Badshah, *J. Photochem. Photobio.*, 2013, **124**, 1.
36. R. Wing, H. Drew, T. Takano, C. Broka, S. Tanaka, K. Itakura and R. E. Dickerson, *Nature*, 1980, **287**, 755.
37. S. K. Konda, C. Kelso, J. Medan, B. E. Sleebs, D. R. Phillips, S. M. Cutts and J. G. Collins, *Org. Biomol. Chem.*, 2016, **14**, 10217.
38. S. G. K. R., B. B. Mathew, C. N. Sudhamani and H. S. B. Naik, *Biomed. Biotech.*, 2014, **2**, 1.
39. J. M. Luco and F. H. Ferretti, *J. Chem. Inform. Comput. Sci.*, 1997, **37**, 392.
40. P. Gramatica and A. Sangion, *J. Chem. Inform. Model.*, 2016, **56**, 1127.
41. E. Pourbasheer, R. Aalizadeh, M. R. Ganjali, P. Norouzi and J. Shadmanesh, *J. Saudi Chem. Soc.,* 2014, **18**, 681.
42. A. Vuorinen and D. Schuster, *Methods San Diego, Calif.*, 2015, **71**, 113.
43. M. De Vivo, M. Masetti, G. Bottegoni and A. Cavalli, *J. Med. Chem.,* 2016, **59**, 4035.
44. B. R. Brooks, C. L. Brooks, A. D. MacKerell, L. Nilsson, R. J. Petrella, B. Roux, Y. Won, G. Archontis, C. Bartels, S. Boresch, A. Caflisch, L. Caves, Q. Cui, A. R. Dinner, M. Feig, S. Fischer, J. Gao, M. Hodoscek, W. Im, K. Kuczera, T. Lazaridis, J. Ma, V. Ovchinnikov, E. Paci, R. W. Pastor, C. B. Post, J. Z. Pu, M. Schaefer, B. Tidor, R. M. Venable, H. L. Woodcock, X. Wu, W. Yang, D. M. York and M.

Karplus, *J. Comput. Chem.*, 2009, **30**, 1545.

45. F. Broccatelli, E. Carosati, A. Neri, M. Frosini, L. Goracci, T. I. Oprea and G. Cruciani, *J. Medic. Chem.*, 2011, **54**, 1740.
46. A. T. Nies and M. Schwab, *Expert Rev. Clinic. Pharmaco.*, 2010, **3**, 707.
47. F. Cheng, Y. Yu, J. Shen, L. Yang, W. Li, G. Liu, P. W. Lee and Y. Tang, *J. Chem. Inform. Mode.,* 2011, **51**, 996.
48. M. Carbon-Mangels and M. C. Hutter, *Mol. Info.,* 2011, **30**, 885.
49. C. Xu, F. Cheng, L. Chen, Z. Du, W. Li, G. Liu, P. W. Lee and Y. Tang, *J. Chem. Info. Model.,* 2012, **52**, 2840.
50. R. L. Marchese Robinson, R. C. Glen and J. B. Mitchell, *Mole. Info.*, 2011, **30**, 443.